Predicting Tumor Response to Radiotherapy Based on Estimation of Non-Treatment Parameters

Yutian Huang
Lafayette College, huangyu@lafayette.edu

Allison L. Lewis
Lafayette College, lewisall@lafayette.edu

Recommended Citation

Predicting Tumor Response to Radiotherapy Based on Estimation of Non-Treatment Parameters

Predicting Tumor Response to Radiotherapy Based on Estimation of Non-Treatment Parameters

Yutian Huang[1], Allison L. Lewis[1],*

*Correspondence:
Prof. Allison Lewis
Dept. of Mathematics
Lafayette College
730 High St.
Easton, PA 18042, USA
`lewisall@lafayette.edu`

Abstract

Though clinicians can now collect detailed information about a variety of tumor characteristics as a tumor evolves, it remains difficult to predict the efficacy of a given treatment prior to administration. Additionally, the process of data collection may be invasive and expensive. Thus, the creation of a framework for predicting patient response to treatment using only information collected prior to the start of treatment could be invaluable. In this study, we employ ordinary differential equation models for tumor growth and utilize synthetic data from a cellular automaton model for calibration. We investigate which parameters have the most influence upon treatment efficacy by comparing parameter distributions associated with treatment outcomes. Additionally, we develop a framework for estimating the probability of observing complete tumor remission following a simulated radiotherapy regimen based only on a patient's non-treatment parameters, so that treatment efficacy could be predicted prior to administration.

Keywords: mathematical oncology, parameter estimation, ordinary differential equations, radiotherapy treatment

1 Introduction

Cancer is the second leading cause of death worldwide. According to the World Health Organization, the year 2018 saw 18.1 million new cancer cases and 9.6 million cancer-related deaths, with approximately 1 in 6 deaths caused by cancer globally [8]. By 2040, the number of new cancer cases and cancer-related deaths per year is expected to rise to 29.5 million and 16.4 million, respectively [7]. Most commonly, cancer results from genetic mutations, often due to environmental causes such as chemicals from tobacco smoke or ultraviolet rays from the sun [6]. These mutations cause abnormal cell division, resulting in mass proliferation and resistance to cell death. Various effective cancer treatments have developed as medical technology improves, but many questions remain regarding which treatments are most effective for which patients. The efficacy of a particular treatment is often difficult to predict prior to treatment administration. As such, it is of great relevance to clinicians to develop a framework in which information collected prior to the treatment period can be used to predict how sensitive a patient will be to a particular therapy—this is the purpose of our investigation.

In this study, we focus primarily on solid tumors (as opposed to other liquid cancers such as lymphomas and leukemias). A tumor is an abnormal mass of tissue that

results from an overabundance of cell growth and division [4]. Normally cells grow and divide to produce new cells in a controlled and orderly manner. In contrast, tumors develop when cells mutate, escape the regular cell cycle, and proliferate unchecked, forming a mass. If a tumor only expands in volume but does not invade nearby tissues, then that tumor is classified as a benign tumor. Benign tumors typically do not grow back once removed. However, malignant tumors—or cancer—can metastasize to other parts of the body and pose great danger to one's health. Common cancer treatments include surgical removal of the tumor from the body, radiotherapy (applying high doses of radiation to kill cancer cells and shrink tumors), chemotherapy (a chemical drug therapy that targets fast-dividing cells), and immunotherapy (which focuses on boosting the immune system to allow it to fight the cancer naturally), among others. Many of these treatments are used in combination—for example, a patient may undergo surgery and then have radiation therapy to target any remaining cells, or they may receive a combination of chemotherapy and immunotherapy to target the cancer from two different perspectives. With the current trend towards personalized medicine, there is a great push for determining which treatment may be most effective for each individual tumor, as opposed to a "one-size-fits-all" approach.

Tumor growth dynamics can be described using a variety of mathematical models. Math models allow sci-

---

[1]Department of Mathematics, Lafayette College, Easton, PA

entists to characterize cancer evolution over time, with opportunities to extrapolate out into the future and simulate how a tumor will behave under different treatment regimens. Tumor evolution has been described using systems of ordinary differential equations, systems of partial differential equations, stochastic models, simulation studies, algebraic models, and even game-theory analysis (see [9] for an overview of the different types of modeling employed and a discussion of how to select an appropriate model for one's objective).

Our purpose in this study is to set the foundation for a framework for predicting how a patient might respond to treatment based only on tumor characteristics and parameter values that can be estimated prior to treatment administration. To demonstrate our procedure, we will employ two ordinary differential equation (ODE) models, described previously in [1]. In this prior work, much analysis was done to investigate when use of these models is appropriate—here, we assume that the model has already been determined to be appropriate for the scenario at hand, and focus on predicting response to radiotherapy. Specifically, we focus on computing the probability of achieving total tumor eradication following a six-week radiotherapy regimen, where this probability is constructed by developing a joint parameter distribution across many simulated patient data sets and extracting the likelihood that a tumor with specific pre-treatment parameter values will respond positively. As part of this process, we first identify which parameters in the model are the most influential "drivers" in a tumor's response to radiotherapy. Though much work remains to be done to prepare this framework for direct use in the clinic, it lays the foundation for the design of a targeted treatment protocol for an individual patient.

We begin in Section 2 by introducing the models we use for demonstration of the framework throughout this research. In Section 3, we use synthetic data to calibrate our models and acquire estimates for the model parameters—in theory, this step would be replaced by clinical data if available. In Section 4, we describe our method for determining which parameters most strongly influence the tumor's response to radiation in isolation. We expand upon this in Section 5 to consider all parameters in conjunction with one another. We estimate a joint parameter distribution from the parameter estimates obtained in Section 3, and use this distribution to compute the probability of observing total tumor eradication when given fixed pre-treatment parameter values, in essence allowing us to predict whether treatment will be effective prior to its administration.

2 Model Formulation

In general, a tumor is composed of a complex, heterogeneous mixture of cells, including regular tumor cells, stromal cells, cancer stem cells, etc. In order to build tangible mathematical models, we are forced to make a number of simplifying assumptions regarding tumor composition. For further discussion of the trade-offs between model complexity and ease of computation, see [1].

In this investigation, we'll consider two different compartment models, which can be used to describe the way in which materials transition between different components of the system. These models were employed in [1] to demonstrate a framework for appropriate model selection and calibration—here, we once again utilize them to illustrate how obtaining estimates for non-treatment parameters prior to treatment administration may help us to predict treatment efficacy.

As a simple case, our first model will assume a homogenous mass of proliferating, viable cells. In contrast, our second model will incorporate an additional layer of complexity, treating the tumor as a two-entity tissue composed of both viable and necrotic cells. In both cases, we then incorporate a radiotherapy treatment model to describe the death rate of tumor cells under radiation.

2.1 One-Compartment ODE Model for Tumor Volume

The one-compartment ordinary differential equation model—henceforth referred to as the OCM—is characterized by a single compartment (V, for "viable") in which all cells reside. If a cell leaves the viable compartment, it immediately exits the system and is no longer tracked by our model. The OCM is built with three assumptions:

1. The tumor spheroid is a homogeneous entity composed entirely of viable, proliferating cells (denoted as V).

2. The growth of the tumor spheroid over time—in the absence of treatment—is described by a logistic growth model with growth rate λ and carrying capacity K.

3. Upon natural cell death, a cell is removed instantaneously from the tumor. The natural death rate of cells is denoted by η.

Figure 1 is a demonstration of the growth dynamics described by the OCM. As per Assumption 2, the OCM is defined by a logistic growth model with growth rate λ and carrying capacity K. In addition, we append the term $-\eta V$ to describe the natural death of tumor cells:

$$\frac{dV}{dt} = \lambda V\left(1 - \frac{V}{K}\right) - \eta V. \tag{1}$$
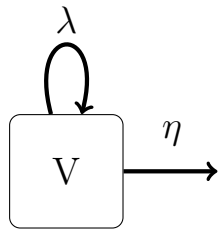
Figure 1: OCM Dynamics Demonstration.

A reformulation of Equation (1) reveals that our model can alternatively be reparameterized in the form

$$\frac{dV}{dt} = AV - BV^2, \qquad (2)$$

where $A = \lambda - \eta$ and $B = \frac{\lambda}{K}$. We prefer this reparameterization, as it decreases the dimensionality of our parameter space from $[\lambda, K, \eta]$ to $[A, B]$. This helps us to avoid issues of parameter identifiability, in the sense that we can no longer observe the same response using two different sets of parameter values. For additional details on assessing both structural and practical identifiability issues with respect to these two models, see [1]. For the remainder of this investigation, any discussion of the OCM will be in reference to Equation (2).

Figure 2 illustrates a simulation of tumor growth modeled by the OCM for a variety of A and B values. The plot on the right displays the impact of varying A on the growth of the tumor for a fixed value of B. It shows that when B remains fixed, the tumor volume is directly proportional to the value of A. The plot on the left shows the impact of varying B on the tumor growth—when A remains fixed, parameter B and the tumor volume are inversely proportional.

2.2 Two-Compartment ODE Model for Tumor and Necrotic Volume

In reality, tumors are far more complex than can be represented by our simple one-compartment model. As a tumor mass grows, it tends to develop a necrotic core composed of cells that have died as a result of being cut off from nutrients and oxygen. As discussed in [1], incorporating a necrotic compartment can drastically improve the accuracy of model predictions in cases where the necrotic core comprises a significant volume of the tumor mass. Therefore, to investigate our framework under a slightly higher degree of complexity, we incorporate a necrotic compartment into our model such that when viable cells die, they remain in the tumor as dead tissue for a time before decaying naturally.

As described above, the two-compartment model (TCM) allows for cells to exist in one of two states—viable
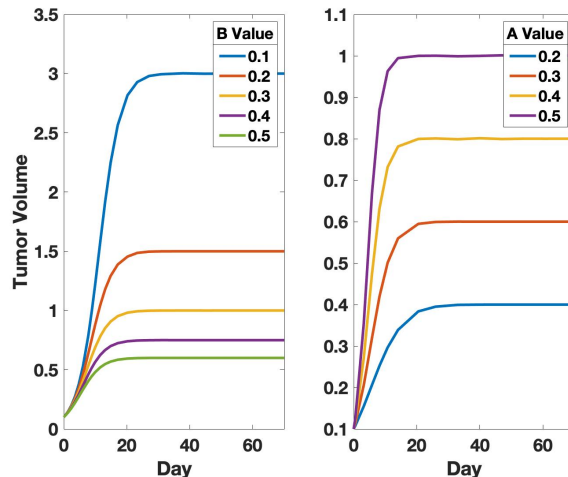

Figure 2: Simulated growth of tumor volume over 70 days, for a sequence of parameter values A and B. On the left, we fix A at 0.3; on the right, we fix B at 0.5.
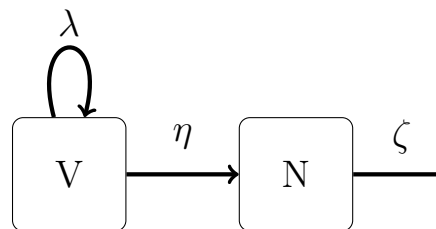
Figure 3: TCM Dynamics Demonstration.

or necrotic—and tracks both populations over time. The model is an extension of the OCM model, with the following assumptions:

1. The tumor spheroid is a heterogeneous body composed of viable (V) and necrotic cells (N).

2. Viable cells are assumed to grow logistically in the absence of treatment with growth rate λ and carrying capacity K.

3. When viable cells die, they convert to necrotic cells—the death rate of viable cells is denoted by η.

4. Necrotic cells decay naturally over time at a rate of ζ. Upon natural decay, the cells are eliminated from our system.

Figure 3 demonstrates the dynamics of the TCM. Taking the assumptions into consideration, we arrive at the following system of ordinary differential equations to de-

scribe the changes in V and N over time:

$$\frac{dV}{dt} = \lambda V \left(1 - \frac{V}{K}\right) - \eta V \qquad (3a)$$

$$\frac{dN}{dt} = \eta V - \zeta N \qquad (3b)$$

As per Assumption 3, the conversion of viable cells to necrotic cells is incorporated via the term ηV—we observe that upon exiting the viable compartment, this quantity immediately enters the necrotic compartment, representing the conversion of viable cells to necrotic material upon cell death.

2.3   The Linear-Quadratic Model for Radiotherapy

We now incorporate a treatment model into our two existing ODE models. In this investigation, we focus on radiotherapy as the treatment protocol.

The radiotherapy (RT) model employed here uses a linear-quadratic equation with radiosensitivity parameters α and β, which represent single-strand and double-strand DNA breaks, respectively [3]. The fraction of cells that survive administration of a dose d of radiation is given by

$$\text{Survival Fraction} = e^{-\alpha d - \beta d^2}. \qquad (4)$$

Since previous work has shown that α and β are not simultaneously identifiable, for the remainder of the investigation we fix $\alpha = 0.14$ and vary β only as outlined in [1]. Namely, we investigate varying radiosensitivity levels indicated by the ratio α/β over a range of $[1, 10]$, where a small ratio (i.e. $\alpha/\beta = 1$) represents higher radiosensitivity due to a larger number of double-strand DNA breaks per single-strand break. Further work is currently being conducted to determine other methods for identifying both α and β uniquely.

For the OCM, the death of viable cells due to radiation manifests as immediate removal of those cells from the system, since there is no mechanism for necrotic material to remain. Thus, within the OCM model, the effect of radiation on the viable cells is incorporated computationally via the mechanism

$$V(t_i^+) = V(t_i^-) \cdot e^{-\alpha d - \beta d^2}, \qquad (5)$$

in which the tumor volume after radiation, $V(t_i^+)$, is equivalent to the volume before, $V(t_i^-)$, multiplied by the survival fraction. In Equation (5), t_i denotes the time at which radiotherapy is delivered and $t_i^{\pm}$ represents the time immediately before and after radiotherapy is administered.
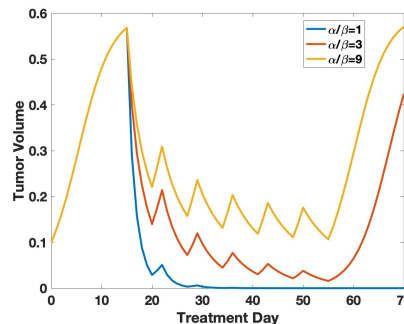

Figure 4: Simulated tumor spheroid growth using the OCM with RT incorporated for varying levels of β and parameter set $[A, B] = [0.3, 0.5]$.

Figure 4 displays the evolution of tumor volume for a simulated tumor spheroid under the effect of radiation with varying radiosensitivity levels (indicated by the value of α/β) using the OCM. For the purpose of this investigation, we utilize a Monday-Friday treatment schedule with a 2 Gy/day dosage for a six week period, starting on Day 15. After the treatment ends, we continue to model the tumor volume for an additional two weeks to simulate a potential regrowth period. In all simulations, we begin with an initial tumor volume of 0.02 cm^3. We observe that in general, larger α/β ratios (representing smaller numbers of double-strand breaks for each single-strand break) result in a weaker response to treatment, as expected.

The incorporation of RT works similarly in the TCM, with the exception that when viable cells are destroyed by radiation, they move into the necrotic compartment as opposed to immediately exiting the system. As such, in Figure 5, we don't observe an instantaneous decline in overall tumor volume, but rather see a spike in the necrotic fraction followed by a delayed decrease in tumor volume as those necrotic cells decay naturally over time.

3   Model Calibration and Parameter Estimation

Our objective of predicting a patient's response to radiotherapy based solely on the values of their non-treatment parameters (i.e. $[A, B]$ in the OCM and $[\lambda, K, \eta, \zeta]$ in the TCM), requires that we estimate those parameters through model calibration. The process of model calibration revolves around identifying those parameter values that yield the best possible fit of the model to a data set. Ideally, we would use experimental data or data collected in the clinic. However, as this type of data is expensive and difficult to come by, we demonstrate our framework here using a synthetic data set generated by a cellular
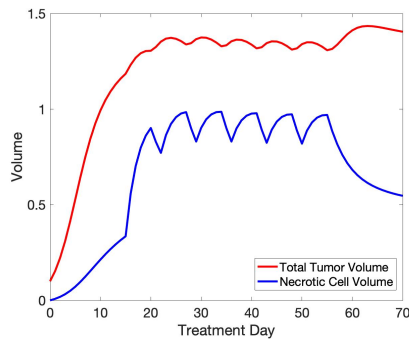
Figure 5: Simulated tumor spheroid growth using the TCM with RT incorporated for $\alpha/\beta = 9$ (i.e. $\beta = 0.0156$) and parameter set $[\lambda, K, \eta, \zeta] = [0.5, 1, 0.12, .07]$.

automaton (CA) model.

Our cellular automaton model—originally developed in [5] and further adapted in [1] to include radiotherapy treatment—incorporates far more complexity by tracking three types of cells (proliferating, quiescent, and necrotic), and simulating oxygen diffusion throughout the tumor. Our CA model is stochastic; that is, cells convert between compartments at random with specified probabilities. The CA model gets its name from the cellular grid setup. Over the course of the algorithm, we track each of the spatial cells and what type of tumor cell they contain at any given time.

The additional complexity of this model allows us to generate synthetic data that is closer-to-reality than that which we might generate from our ODEs. Throughout this investigation, we treat this synthetic data as "truth". Using this CA model, we generated 1000 sets of synthetic tumor spheroid data by varying the parameters that control the mean and standard deviation of the cell cycle duration (effectively controlling the natural death rate), the oxygen thresholds for determining the conversion from proliferating-to-quiescent and quiescent-to-necrotic, the radiosensitivity parameter β, and the probability of necrotic cell removal at each iteration (which controls the decay rate of the necrotic material). Table 1 lists the parameter ranges and default values used for generation of the synthetic tumor data.

Following generation of our synthetic data, we then calibrate the model using the MATLAB function `fmincon`, which minimizes the sum-of-squares of the differences between the data and the model predictions under a set of constraints (here, we constrain all parameter values to be at least zero, so as to be physically reasonable). As a result, we finish with 1000 sets of parameter estimates chosen to yield the best possible fits to the 1000 synthetic data sets.

We note that the OCM is not bi-stable; that is, the only stable equilibrium occurs when the tumor reaches carrying capacity. The zero state (tumor eradication) is an unstable equilibrium—unless the model reaches *exactly* zero computationally, the tumor will regrow in the simulation. Since, computationally speaking, the ODE solver nearly always reports small fractions of cells when close to tumor eradiction instead of a strictly zero volume, we never observe OCM simulations where tumors remain eradicated after treatment is complete. Biologically speaking, we know that when a tumor is reduced to a small enough volume, the immune system is capable of clearing the remainder of the tumor. As such, we model this phenomenon in the OCM by introducing an immune threshold—a value below which we set the tumor volume to zero to represent total eradication. This immune threshold was determined to be 4.4913×10^{-4} cm^3, and was estimated by comparing outcomes (eradicated vs. not-eradicated) between the OCM and CA models for each of the 1000 simulated spheroids and choosing the threshold value that would maximize the number of outcome matches between the two. The OCM model was then recalibrated with the immune threshold incorporated computationally to arrive at the final parameter estimates. Though the TCM is bistable and capable of producing long-term eradicated behavior, we still incorporated this threshold when calibrating the TCM in order to mimic the behavior of the immune system at a rudimentary level. Further work is currently being done to investigate other means by which we can incorporate the immune system without making our models too complex for this analysis.

Figure 6 illustrates examples of fitting the one- and two-compartment models to synthetic data generated by the cellular automaton model. In our OCM example, the tumor volume decreases to zero by Day 40. This indicates that the tumor is completely eradicated at this point. As a result, the tumor volume remains at zero for the rest of the simulation period, as enforced by our incorporation of the immune threshold. In our TCM example, generated using a different sample data set, the tumor volume reaches its lowest point around Day 56 (the final day of treatment) but then increases. Since the tumor is not completely eradicated during the six-week treatment period, we observe a period of regrowth following the completion of the radiotherapy regimen.

4 Investigating Parameters with Respect to Treatment Outcome

Having completed our parameter estimation procedure, we now move to determining which parameters are most influential in determining how a tumor will react to radiotherapy. Throughout this section, we consider each

Table 1: A summary of the parameters used in the CA model and their default values (and ranges, where relevant). Default parameter values were estimated using experimental data from the prostate cancer cell line, PC3, in [5].

Parameter	Description	Value	Units
l	Cell size	0.0018	cm
L	Domain length	0.36	cm
$\bar{\tau}_{cycle}$	Mean (std. dev.) cycle time	$[15, 30]$ $([0, 5])$	hr
c_∞	Background O_2 conc.	2.8×10^{-7}	mol/cm^3
D	O_2 diffusion constant	1.8×10^{-5}	cm^2/s^1
c_Q	O_2 conc. threshold for viable cells	$[0.5, 0.8]$	—
c_N	O_2 conc. threshold for quiescent cells	$[0.5, c_Q]$	—
κ_V	O_2 consumption of viable cells per time step	257.24	—
κ_Q	O_2 consumption of quiescent cells per time step	128.57	—
p_{NR}	Rate of lysis of necrotic cells	$[.001, .01]$	1/hr
β	Radiosensitivity for double-strand breaks	$[.014, .14]$	1/Gy^2
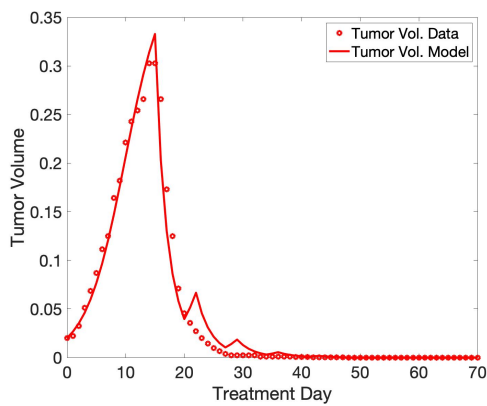
(a)
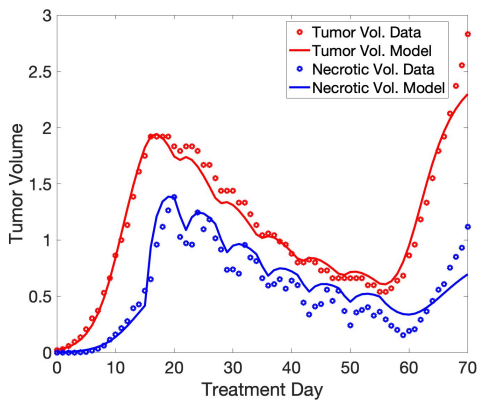
(b)

Figure 6: (a) OCM fit to CA data for a sample spheroid. The final estimated parameter set is $[A, B, \beta] = [0.30013, 0.74326, 0.094226]$. (b) TCM fit to CA for a sample spheroid, with the final estimated parameter set $[\lambda, K, \eta, \zeta, \beta] = [0.5004, 2.000, 0.088744, 0.15414, 0.065836]$.

parameter in isolation, temporarily disregarding any correlation between them. Our goal is to gain some preliminary insight as to which parameters may have the most impact on response to RT to further motivate our later investigation. We recognize that response to RT may in fact be driven by combinations of parameters working in tandem, and address this further in Section 5. This section is specifically intended to see whether we can rule out any parameters as being influential in determining chances of eradication via a hypothesis testing framework.

We separate the 1000 spheroids synthesized in Section 3 into two clusters depending on whether or not their tumor volumes reach zero during the treatment period. We note that while biologically speaking, a spheroid residing in the non-zero cluster doesn't necessarily indicate that it hasn't responded *positively* to RT, mathematically speaking, we must choose a numerical cutoff for clustering the spheroids. Zero, in this case, makes the most sense as a break point.

In order to determine the influential parameters, we form and compare each parameter's distributions between the two clusters. For each pair of distributions (representing a single parameter across the two groups), we compare their means and variances using hypothesis tests to determine whether a parameter's distributions differ by cluster. Performing a hypothesis test gives us a way to test an assumption about the value of an unknown parameter. We frame our test using a null hypothesis (H_0), the claim that is initially assumed to be true, and an alternative hypothesis (H_a), representing a contrasting claim. Based on our sample, we gather evidence to either reject the null claim (in which case we have evidence in support of the alternative hypothesis) or fail to reject the null. The decision about whether or not to reject the null can be made in one of two ways; either we can compare a computed test statistic (a measure that helps us distinguish

between normal and abnormal sample results under the assumption that the null claim is true) to a rejection region, or compare the p-value to a pre-specified threshold. A p-value represents the probability of obtaining a test statistic value that is at least as extreme as the observed value from our sample under the assumption that the null hypothesis is true. The smaller the p-value, the stronger the evidence we have in support of our alternative hypothesis. Therefore, we reject H_0 when the p-value is less than or equal to the pre-specified significance level; else, we fail to reject H_0 and conclude that we have insufficient evidence to suggest that the null claim is not true. For further information regarding the hypothesis testing framework, we recommend [2].

In this investigation, we utilize hypothesis tests to compare distributions across clusters with respect to both their means and variances, since these are two major components of a distribution representing center and spread. If either the center or spread of the two distributions being compared is found to be significantly different, we have evidence to suggest that there is a relationship between the cluster (eradicated vs. not-eradicated) and that parameter, indicating that the parameter in question cannot be ruled out as influential in determining a tumor's response to radiotherapy. The boxplots shown in Figures 7 and 8 visualize the parameter distributions by cluster for both models. Excluding outliers, all parameter distributions appear to be relatively normal. For all hypothesis tests, we utilize a significance level of $\alpha = 0.01$.

To compare the means of the distributions, we employ a two-sample t-test. Our null hypothesis states that the two clusters come from independent, normally distributed random samples with equal means, or $H_0 : \mu_1 - \mu_2 = 0$, where μ_1 and μ_2 represent the true but unknown means of the parameter distributions for the eradicated and not-eradicated tumors, respectively. Alternatively, our contrasting claim is $H_a : \mu_1 - \mu_2 \neq 0$; that is, there is a difference between the two true means. The results of the mean tests for the OCM and TCM are shown in Tables 2 and 3.

For the OCM, we find evidence that the true means differ between clusters for all three parameters, $[A, B, \beta]$, as evidenced by observing p-values for all three tests that are less than $\alpha = 0.01$. Similarly, in the TCM, we find evidence that the true means differ between groups for all parameters $[\lambda, K, \eta, \zeta, \beta]$. This evidence is further supported by our construction of 99% confidence intervals to capture the true difference in means (eradicated minus not-eradicated). In all cases, we find that the confidence intervals do not contain zero, suggesting that zero is not a plausible value for $\mu_1 - \mu_2$.

To compare the variances, we employ the two-sample F-test, which compares the ratio of sample variances to determine whether it is plausible that the underlying pop-
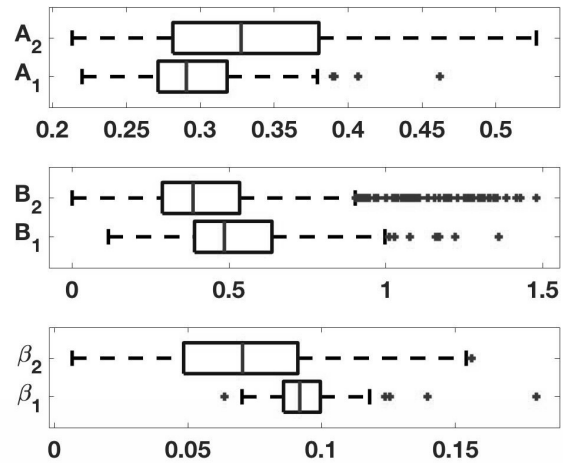

Figure 7: Boxplots of the OCM parameter clusters. Group 1 represents the eradicated cluster and Group 2 represents the non-eradicated cluster.
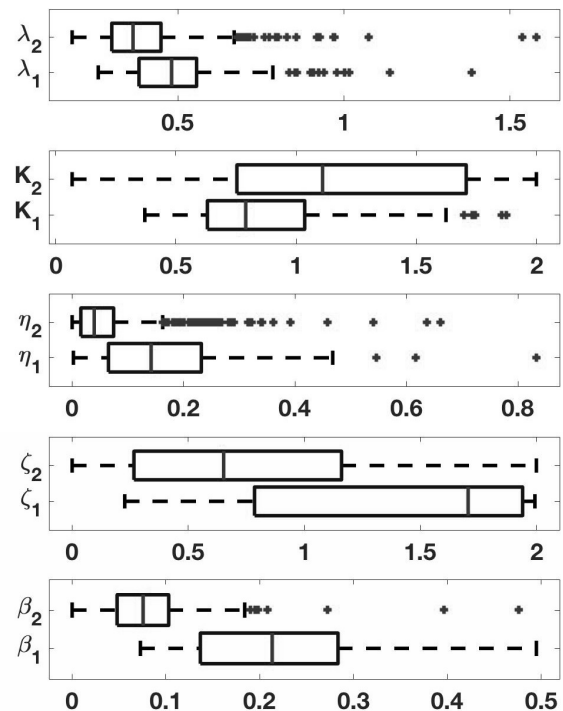

Figure 8: Boxplots of the TCM parameter clusters. Group 1 represents the eradicated cluster and Group 2 represents the non-eradicated cluster.

Table 2: Hypothesis test results and confidence intervals for the difference in the means of OCM parameter distributions generated from the two-sample t-test.

Parameter	p-value	CI for Mean
A	3.9437×10^{-21}	$(-0.0466, -0.0276)$
B	4.2242×10^{-6}	$(0.0427, 0.1475)$
β	3.8169×10^{-39}	$(0.0178, 0.0256)$

Table 4: Hypothesis test results and confidence intervals for the ratio of variances of TCM parameter distributions generated from the two-sample F-test.

Parameter	p-value	CI for Variance
A	1.7979×10^{-14}	$(0.2465, 0.4703)$
B	0.0136	$(0.5318, 1.0148)$
β	4.8101×10^{-25}	$(0.1558, 0.2973)$

Table 3: Hypothesis test results and confidence intervals for the difference in the means of TCM parameter distributions generated from the two-sample t-test.

Parameter	p-value	CI for Mean
λ	3.9436×10^{-10}	$(0.0760, 0.1718)$
K	1.4749×10^{-16}	$(-0.4249, -0.2347)$
η	4.2715×10^{-14}	$(0.0705, 0.1331)$
ζ	1.0369×10^{-19}	$(0.4712, 0.7804)$
β	3.6572×10^{-26}	$(0.1308, 0.1932)$

Table 5: Hypothesis test results and confidence intervals for the ratio of variances of TCM parameter distributions generated from the two-sample F-test.

Parameter	p-value	CI for Variance
λ	2.5432×10^{-10}	$(1.5729, 3.2249)$
K	3.9556×10^{-8}	$(0.3036, 0.6225)$
η	3.5832×10^{-24}	$(2.3934, 4.9072)$
ζ	0.1408	$(0.8666, 1.7768)$
β	4.6439×10^{-93}	$(6.6140, 13.5608)$

ulation variances are equal. Our null hypothesis is that the two parameter distributions have the same underlying population variances; $H_0 \colon \sigma_1^2/\sigma_2^2 = 1$. The alternative hypothesis is given by $H_a \colon \sigma_1^2/\sigma_2^2 \neq 1$. The p-values generated from the variance tests are shown for both models in Tables 4 and 5. For parameters A and β in the OCM, and parameters $[\lambda, K, \eta, \beta]$ in the TCM, we conclude that we have sufficient evidence to suggest a difference in the underlying population variances, as shown by the p-values that are less than $\alpha = 0.01$. In contrast, the confidence intervals for B in the OCM and ζ in the TCM both include 1, suggesting that it is plausible that the underling population variances are equivalent across clusters for these two parameters.

Combining the results of the t- and F-tests for the OCM, we observe that the two sets of parameter clusters for A and β have significantly different means and variances. Even though there is not sufficient evidence to indicate that the variances of the B clusters are unequal, we have evidence suggesting that the means of these clusters are different. Since the parameter distributions of the eradicated and not-eradicated tumors for A, B and β are all significantly different, we cannot rule out A, B or β as potential drivers in a tumor's response to radiotherapy. However, further investigation must be done to determine whether each of these parameters is in fact influential, or whether there is an underlying confounding effect; i.e. a correlation between two different parameter values is driving the significant test results for one parameter. Additionally, we note that hypothesis testing is vulnerable to manipulation by sample size; for a large enough sample size, any difference between samples can

be concluded to be significant. As we are working with sample sizes of 152 and 848 in the OCM, and 119 and 881 in the TCM (Groups 1 and 2, respectively), we must be cautious when interpreting these seemingly significant results.

Moving to the TCM analysis, we observe again that the clusters of all TCM parameters have significantly different underlying distributions. As a result, we conclude that λ, K, η, ζ, and β are all still candidates when it comes to determining which parameters are driving a tumor's response to radiotherapy. Section 5 will delve into the relationships between these parameters to determine which parameters are the *most* influential.

5   Predicting Response to RT Using Non-Treatment Parameters

Ideally, we would like to be able to predict the efficacy of a particular treatment prior to the administration of the treatment regimen, allowing clinicians to compare and contrast different treatment methods to choose the one that will most benefit the particular patient. Since we are interested in predicting the probability of a tumor being eradicated prior to administering treatment, we turn our focus to analyzing how non-treatment parameters (A and B for the OCM model and λ, K, η and ζ for the TCM model) may help us to predict how sensitive a tumor will be to radiation, with the assumption that β (the radiosensitivity parameter) is as of yet unknown.

Unlike in Section 4, where we consider the parameters in isolation and conduct hypothesis tests on each to determine which may be candidates for influential parameters, in this section, we consider this question more generally. Specifically, we investigate how non-treatment parameters work together in tandem to drive response to radiotherapy. To achieve this, we first return to the existing parameter combinations generated through our model calibration procedure in Section 3. We create a matrix of all 1000 parameter combinations, including β, and use this matrix to estimate a joint multivariate density across all model parameters using the MATLAB `mvksdensity` command. Then, for a grid of non-treatment parameter values, we consider the conditional densities for β, the treatment parameter. For instance, in the OCM, we can transition from the total joint density $f(A, B, \beta)$ to a conditional distribution $f(\beta \mid A = a, B = b)$ by fixing $[A, B] = [a, b]$ and analyzing the distribution of values observed in β for this fixed pair [2].

Next, we estimate the probability of obtaining an eradicated tumor using the conditional distributions for β. For each fixed pair $(A = a, B = b)$ under consideration, we find the threshold value of β for which a tumor with parameter pair (a, b) would be eradicated, if such a threshold exists. By numerically integrating the portion of the conditional distribution for which the tumor would be eradicated and dividing by the total area of the conditional distribution, we can estimate the probability of achieving total tumor eradication under these conditions. That is, by exploiting the information we gained in Section 3 about which parameters values are likely to occur in combination with one another, we can estimate how likely a spheroid is to undergo total eradication by knowing only the values of its non-treatment parameters A and B. For the TCM, we can conduct a similar analysis to predict the likelihood of tumor eradication given a fixed set of $[\lambda, K, \eta, \zeta]$ values.

5.1   One-Compartment Model Results

In Figure 9, we present the results for the one-compartment model. Figure 9(a) plots a set of possible parameter pairs (a, b) and their corresponding β thresholds in a 3-dimensional scatterplot, allowing us to see the relationship between a non-treatment parameter pair (a, b) and the β threshold value that would be required to eradicate the tumor. As can be observed from the figure, parameter A is much more highly correlated with the β threshold than B; that is, the choice of an eradication threshold value is closely tied to the net growth rate of the tumor and less impacted by the carrying capacity.

Figure 9(b) demonstrates the probability of obtaining an eradicated tumor on a 2-dimensional heat map. From the figure, we find that both A and B are influential
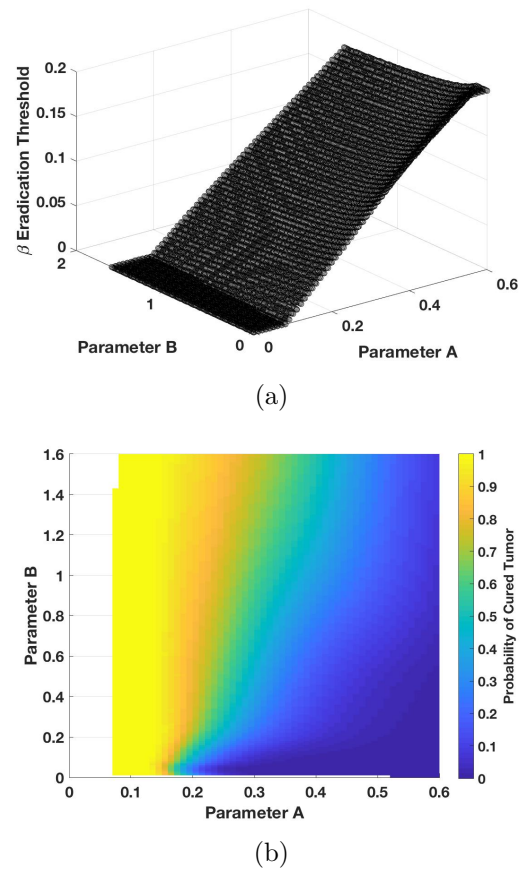

(a)

(b)

Figure 9: (a) OCM scatterplot demonstrating the correlation between the non-treatment parameters A, B, and the β threshold. (b) OCM heat map describing probability of tumor eradication as a function of non-treatment parameters.

in regards to the probability of total tumor eradication, though A is much more so. In general, the larger the ratio of A/B, the more likely that a tumor spheroid cannot be eradicated. To connect this result to the underlying biology, we recall that in the reformulation of the OCM, $A = \lambda - \eta$, representing the net growth rate of a tumor. For a fixed value of B, a larger net growth rate A will result in a decreased likelihood of tumor eradication. We also observe that the dependence of tumor eradication probability on B seems to increase slightly as A increases. Recall that in the OCM reformulation, B represents the ratio of the growth rate (λ) of a tumor to the carrying capacity (K). Thus, our figure suggests that the larger the net growth rate, the greater the dependence of the eradication probability on the carrying capacity—this is unsurprising, as only tumors with large net growth rates are likely to reach their carrying capacity in the short term.

5.2   Two-Compartment Model Results

Figure 10(a) illustrates possible values of the four non-treatment parameters—$\{\lambda, K, \eta, \zeta\}$—with respect to the β thresholds that would be required to achieve eradication for the two-compartment model. We observe a positive correlation between the growth rate λ and the required β threshold; as the growth rate of a tumor increases, a more drastic radiotherapy response is required to eliminate the tumor. On the contrary, the natural death rate of viable cells, η, and the β threshold are negatively correlated; larger death rates may be matched with smaller radiotherapy responses and still achieve a positive outcome, since tumor cells are dying more rapidly of their own accord. It can be observed that K and ζ are not correlated with the β threshold values.

Figure 10(b) illustrates the expected probability of tumor eradication under each of the two-dimensional projections of the TCM non-treatment parameter space. We note that there are four non-treatment parameters for the TCM model, $[\lambda, K, \eta, \zeta]$. To incorporate the effects of all four, we project into two-dimensional parameter regimes and average the probability of eradication over all values of the remaining two parameters for each pair under consideration. This allows us to account for potential correlations between parameters and determine which parameters are truly responsible for influencing the probability of achieving complete tumor eradication.

Analyzing all six projections in unison, we quickly observe that the main "drivers" in the function are λ and η; any noticeable differences with respect to the average probability of tumor eradication occur in accordance with changes in these two parameters. Perhaps the most interesting heat map is that which projects into the (λ, η) space. Here we see that the probability of eradication decreases with increasing λ and decreasing η. Biologically, this agrees with our intuition; the probability of eradicating the tumor should increase proportionally with an increasing death rate of viable cells (η), but should be indirectly related to the growth rate (λ).

When observing any of the maps that project into the K or ζ spaces, we see that there is very little relationship between eradication probability and these two parameters. Indeed, the (K, ζ) map shows a stable average probability of roughly 0.58, regardless of the values of K and ζ. We conclude that K and ζ are relatively uninfluential in determining a spheroid's sensitivity to radiation, and deduce that the significant results seen with respect to these two parameters in Section 4 were in fact due to correlations with λ, η, and/or β. For example, if large values of K were likely to exist only in conjunction with large values of η, as determined by the model calibration procedure, then our clustering of spheroids with respect to eradication would result in two K clusters with signif-
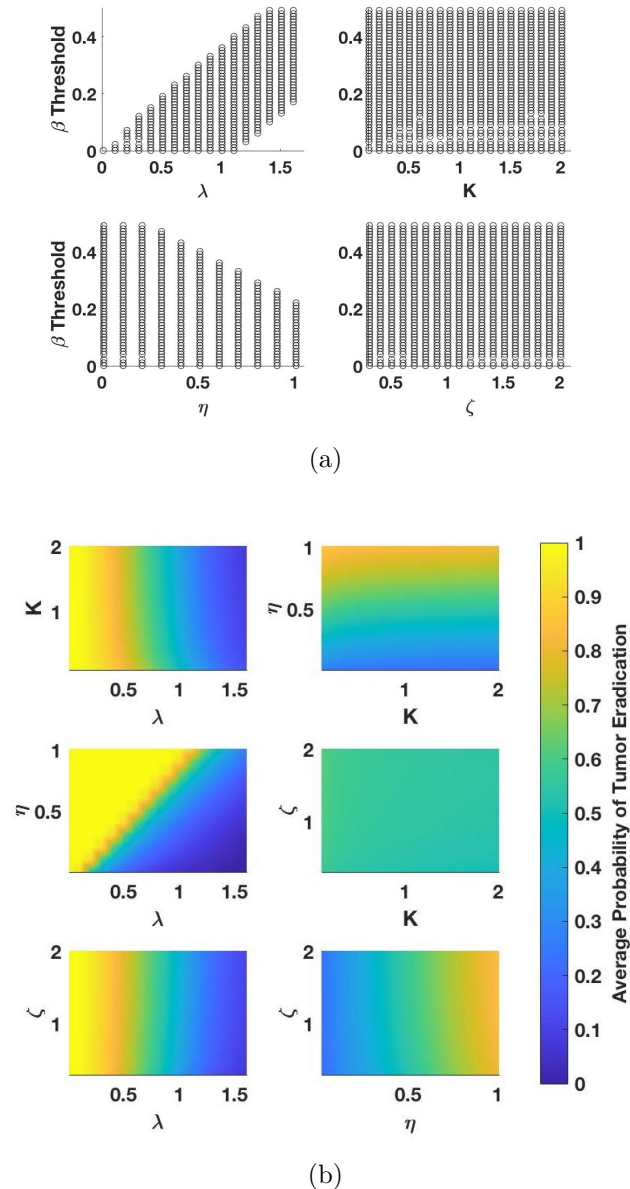

(a)

(b)

Figure 10: (a) TCM scatterplots demonstrating the correlation between the non-treatment parameters λ, K, η, ζ, and the β threshold. (b) TCM heat maps describing probability of tumor eradication as a function of non-treatment parameters.

icantly different means, despite the fact that K was not the parameter responsible for prompting that behavior.

In summary, we conclude that the non-treatment parameters λ and η are most influential when it comes to predicting the probability of achieving total eradication. That is, if one could determine prior to treatment that a particular spheroid possessed a large value of λ and a small value of η, one could be reasonably confident that the proposed treatment regimen would be effective. In contrast, determining the values of K and/or ζ in advance of treatment administration does not help one to predict the efficacy of the treatment.

6   Conclusion

Cancer is a devastating and stubborn disease. Even in the era of rapid development of medical technology, scientists are still devoted to discovering and improving the most effective treatments for tumor eradication. The recent trend towards personalized medicine supports the the design of treatments tailored to individuals; however, this approach is often inefficient with respect to both time and expense. Given the promising future of personalized medicine, we conducted this research with the goal of laying the foundation for a framework in which one could predict the efficacy of treatment for an individual based solely on the values of their non-treatment model parameters, obtained from a model calibration performed prior to treatment administration.

With the use of hypothesis testing conducted on parameter distributions clustered by treatment outcome, we are able to investigate how different parameter values may yield different results with regards to treatment outcomes. In addition, by utilizing conditional distributions for treatment parameters at fixed values of non-treatment parameters, we are able to make predictions about the probability of tumor eradication using only non-treatment parameter values. For the OCM, we discover that A, the net growth rate of a tumor, has the most impact on the eradication probability. For the TCM, we find that λ and η—representing the growth and natural death rates of viable tumor cells, respectively—are ultimately responsible for determining the probability of successful eradication.

As experimental data was not available for our research, we utilized synthetic data generated from a cellular automaton model. As a result, additional validation and verification would be required before any direct conclusions could be drawn at the clinical level. Specifically, ongoing work is being conducted with respect to determining conditions under which non-treatment parameters can be uniquely identified using only pre-treatment data, identifying how much data must be available in order to accurately estimate these parameters, and deciding how to choose an appropriate level of model complexity for any given situation. Regardless, this work lays the foundation for a framework that could eventually assist in the decision-making process in a clinical setting.

Author Contributions

Y. Huang completed this research under the direction of A. Lewis as part of the Lafayette College EXCEL Scholar Program in Summer 2020. Y.H.: code development, analysis of results, manuscript writing. A.L.: conceptualization, data curation, assistance with code development, analysis, and manuscript writing.

References

[1] Cho, H., Lewis, A. L., Storey, K. M., et al. (2020) A Framework for Performing Data-Driven Modeling of Tumor Growth with Radiotherapy Treatment. Using Mathematics to Understand Biological Complexity. Association for Women in Mathematics. Series 22.

[2] Devore, J. L. and Berk, K. N. (2012). *Modern Mathematical Statistics with Applications*. Springer.

[3] Enderling, H., Chaplain, M. A. J., and Hahnfeldt, P. (2010). Quantitative modeling of tumor dynamics and radiotherapy. *Acta Biotheoretica*, 58(4):341–353.

[4] Healio (4 Apr. 2017). What Is a Tumor? `www.healio.com/news/hematology-oncology/20120331/what-is-a-tumor`.

[5] Kannan, P., Paczkowski, M., Miar, A., et al. (2019). Radiation resistant cancer cells enhance the survival and resistance of sensitive cells in prostate spheroids. *bioRxiv*. doi: 10.1101/564724.

[6] National Cancer Institute (9 Feb. 2015). What Is Cancer? *Understanding Cancer*. `www.cancer.gov/about-cancer/understanding/what-is-cancer`.

[7] National Cancer Institute (25 Sept. 2020). Cancer Statistics. *Understanding Cancer*. `www.cancer.gov/about-cancer/understanding/statistics`.

[8] World Health Organization (12 Sept. 2018). *Cancer*. `www.who.int/news-room/fact-sheets/detail/cancer`.

[9] Yin, A., Moes, D.J.A.R., van Hasselt, J.G.C., Swen, J.J., and Guchelaar, H.-J. (2019). A Review of Mathematical Models for Tumor Dynamics and Treatment Resistance Evolution of Solid Tumors. *CPT: Pharmacometrics Syst. Pharmacol.*, 8(10):720–737.